ORIGINAL ARTICLE
Clin Endosc 2021;54:222-228
https://doi.org/10.5946/ce.2020.090
Print ISSN 2234-2400 • On-line ISSN 2234-2443

CLINICAL ENDOSCOPY

Open Access

Histological Architecture of Gastric Epithelial Neoplasias That Showed Absent Microsurface Patterns, Visualized by Magnifying Endoscopy with Narrow-Band Imaging

Kenta Chuman[1,2], Kenshi Yao[1], Takao Kanemitsu[1], Takashi Nagahama[1], Masaki Miyaoka[1], Haruhiko Takahashi[2], Kentaro Imamura[3], Rino Hasegawa[1], Toshiharu Ueki[3], Hiroshi Tanabe[3], Seiji Haraoka[2] and Akinori Iwashita[2]

Departments of [1]Endoscopy, [2]Pathology, and [3]Gastroenterology, Fukuoka University Chikushi Hospital, Fukuoka, Japan

Background/Aims: The objective of this study was to elucidate the histological structure of the absent microsurface patterns (MSPs) that were visualized by magnifying endoscopy with narrow-band imaging (M-NBI).
Methods: The study included consecutive gastric epithelial neoplasias for which M-NBI findings and histological findings could be compared on a one-to-one basis. The lesions were classified as absent MSPs and present MSPs based on the findings obtained using M-NBI. Of the histopathological findings for each lesion that corresponded to M-NBI findings, crypt opening densities, crypt lengths, crypt opening diameters, intercrypt distances, and crypt angles were measured and compared.
Results: Thirty-six lesions were included in the analysis; of these, 17 lesions exhibited absent MSP and 19 lesions exhibited present MSP. Comparing the histological measurements for absent MSPs vs. present MSPs, median crypt opening density was 0.9 crypt openings/mm vs. 4.8 crypt openings/mm (p<0.001), respectively. The median crypt length, median crypt opening diameter, median intercrypt distance, and median crypt angle were 80.0 μm vs. 160 μm (p<0.001), 40.0 μm vs. 44.2 μm (p=0.09), 572.5 μm vs. 166.7 μm (p<0.001), and 21.6 degrees vs. 15.5 degrees (p<0.001), respectively.
Conclusions: Histological findings showed that lesions exhibiting absent MSPs had lower crypt opening density, shorter crypt length, greater intercrypt distance, and larger crypt angle. **Clin Endosc 2021;54:222-228**

Key Words: Gastric cancer; Magnifying endoscopy; Narrow-band imaging

INTRODUCTION

In recent years, magnifying endoscopy with narrow-band imaging (M-NBI) has permitted the diagnosis of small, flat early gastric cancers, which are difficult to diagnose using conventional white-light endoscopy.[1] In addition, the results of numerous exploratory studies examining the relationship between magnifying endoscopy findings and histological findings have been reported.[2-9] However, the viewing conditions in these investigations, such as the degree of magnification obtained by magnifying endoscopy, have not been uniform, and no studies have reported on a one-to-one correspondence between the site visualized by magnifying endoscopy and the histopathological findings. Uchita et al. reported that the diagnostic accuracy of magnifying endoscopy differs according to the viewing conditions,[10] and that it is ideal to establish uniform viewing conditions at maximum magnification. Major advances in endoscopic diagnosis have been achieved because the morphological features have been confirmed histologically. With magnifying endoscopy, however, the region observed is more minute, and a one-to-one correspondence is therefore required when examining the histological findings for the observed sites. Consequently, Yao et al. reported that in order to match resected gastric epithelial tumor specimens to

Received: April 4, 2020 **Revised:** May 19, 2020
Accepted: May 25, 2020

Correspondence: Kenshi Yao
Department of Endoscopy, Fukuoka University Chikushi Hospital, 1-1-1 Zokumyoin, Chikushino, Fukuoka 818-8502, Japan
Tel: +81-92-921-1011, **Fax:** +81-92-929-2630, **E-mail:** yao@fukuoka-u.ac.jp
ORCID: https://orcid.org/0000-0003-0863-3649

endoscopy images, it is important to record images of indices that provide orientation and markings that serve as landmarks before the resection is performed.[11] In addition, Doyama et al. described a method of marking that indicates the region of interest on a lesion observed by magnifying endoscopy.[12]

Furthermore, Kanesaka et al. reported a significantly higher proportion of undifferentiated-type adenocarcinomas when absent microsurface patterns (MSPs) account for 50% or more of the regions of early gastric cancers, as observed by magnifying endoscopy.[4] This suggests that it is possible to diagnose undifferentiated-type adenocarcinomas endoscopically before surgery. However, it is not known why these cancers have absent MSPs.

Given this background, the present study aimed to elucidate the mechanism that results in absent MSPs, as observed by magnifying endoscopy. To accomplish this, histological findings that reliably matched the sites of the findings obtained by M-NBI under uniform viewing conditions, were compared with those findings on a one-to-one basis, and the differences in the histological findings between lesions that exhibit absent MSPs and those that exhibit present MSPs were examined.

MATERIALS AND METHODS

The study was a single-center, retrospective, observational study and was conducted after being approved by the ethics committee of Fukuoka University (R18-050).

Inclusion criteria

Of the early gastric cancer lesions treated at Fukuoka University Chikushi Hospital between August 2015 and January 2018, the consecutive lesions for which all of the following conditions were fulfilled were included in the study: the lesion was a gastric epithelial neoplastic lesion (carcinoma and adenoma), where two marks demarcating the region of interest were added and could be identified (Fig. 1A). The area between the two marks was observed by magnifying endoscopy at maximum magnification (Fig. 1B, C), and a tissue section was prepared from a specimen site between the two marks (Fig. 1D-F).

Exclusion criteria

Lesions for which magnifying endoscopic imaging was not performed at maximum magnification and those that could not be examined histopathologically due to factors such as severe tissue crushing were excluded.

Endoscopic procedures

After obtaining written informed consent from the patient, endoscopy was performed by three experienced endoscopists (KY, TN, and MM). For all lesions, M-NBI was performed using a magnifying endoscope (GIF-Q290Z or GIF-Q240Z; Olympus Medical System Co., Tokyo, Japan) and an endoscopy system (EVIS LUCERA ELITE; Olympus Medical System) with a black soft hood (MAJ1989; Olympus Medical System) attached to the endoscope tip. The tip was brought to a distance of 2 mm from the mucosa; this distance was maintained, and images obtained at maximum magnification were used. Details of the procedure were described previously.[13]

Determining MSP using M-NBI: definition of absent MSPs vs. present MSPs

Lesions included in the study were classified as belonging to either the present MSP group (Fig. 2A) or absent MSP group (Fig. 2B) based on the surface microstructure in the region of interest, as observed by magnifying endoscopy. Present MSP was defined as such when the marginal crypt epithelium could be observed in three-quarters or more of the region of interest. Absent MSP was defined as such when the marginal crypt epithelium could be observed in only one-quarter or less of the region of interest. The MSP was determined by an experienced endoscopist (KY) who was blinded to the histological findings.

Histopathological assessment

The following histopathological measurements were performed for the histopathological findings corresponding to the region of interest, as observed by magnifying endoscopy: (1) crypt opening density, determined by dividing the number of crypt openings by the distance examined (Fig. 3A); (2) crypt length, the distance from the center of the crypt opening to the deepest part of the crypt (Fig. 3B); (3) crypt opening diameter, the distance across the crypt opening (Fig. 3C); (4) intercrypt distance, the distance between crypts (Fig. 3D); and (5) crypt angle, the angle between a line connecting the center of the crypt opening to the deepest part of the crypt, and a line drawn vertically from the crypt opening to the muscularis mucosae (Fig. 3E). The histopathological measurements were performed by an independent single pathologist (KC) who was blinded to the endoscopic findings. The tissue-type classification was performed according to the Japanese Classification of Gastric Carcinomas (14th edition).[14]

Endpoints

The following were determined:

1) Differences in histological measurements between the

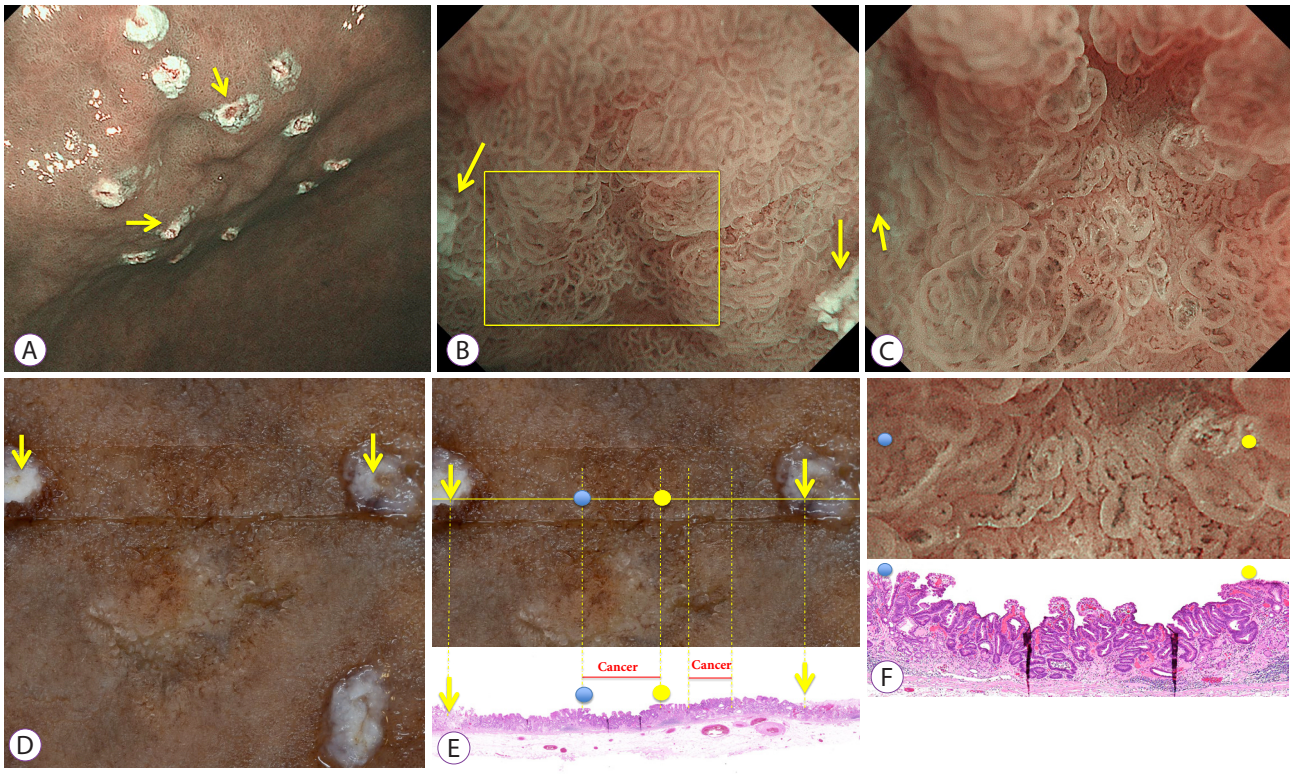

Fig. 1. Correspondence between the regions of interest in images obtained by magnifying endoscopy with narrow-band imaging (M-NBI) and matching histological findings. (A) Image obtained by M-NBI. In addition to marks added before endoscopic submucosal dissection (ESD) to indicate the extent of the resection, M-NBI was used to place marks at two points on either side of the lesion. (B) M-NBI: weak magnification. Magnified observation of the area between the two marks was performed by M-NBI (the arrows indicate the marks). (C) M-NBI: maximum magnification. Magnified observation was performed for the area enclosed by the square shown in (B), and the recorded endoscopic findings were used (arrows indicate marks). (D) Formalin-fixed specimen after ESD. After the lesion was resected by ESD, stretched, and fixed in place on a rubber plate with pins, the two marks made before ESD were identified. A cut was made between the two marks, sections were prepared, and hematoxylin-eosin staining was performed. (E) Post-ESD formalin-fixed specimens (top) matched with histological findings (bottom). Marks on the prepared sections were first identified, and histological findings for the area between the marks were observed (arrows indicate marks). Blue and yellow circles on the resected specimen at the top correspond, respectively, to the blue and yellow circles in the histological findings on the bottom. (F) Correspondence between M-NBI (maximum magnification, top) and histological findings (bottom). Histological findings corresponding to the region of interest in the image obtained by M-NBI were identified using the two marks from before the resection (C) and the two marks in the histological findings (E). Blue and yellow circles on the image obtained by M-NBI at the top correspond, respectively, to the blue and yellow circles in the histological findings on the bottom.

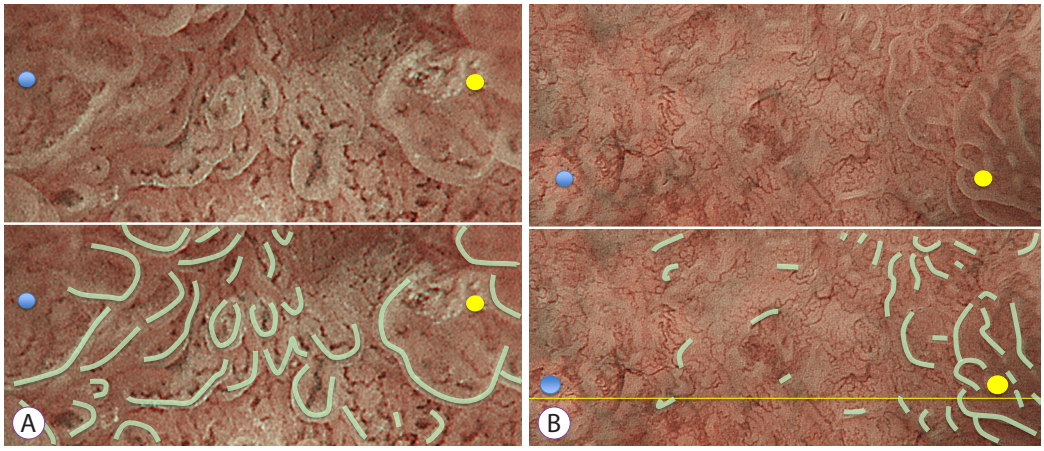

Fig. 2. Assessment of microsurface patterns (MSPs). (A) Present MSPs (bottom: marginal crypt epithelium traced with gray line). (B) Absent MSPs (bottom: marginal crypt epithelium traced with gray line).

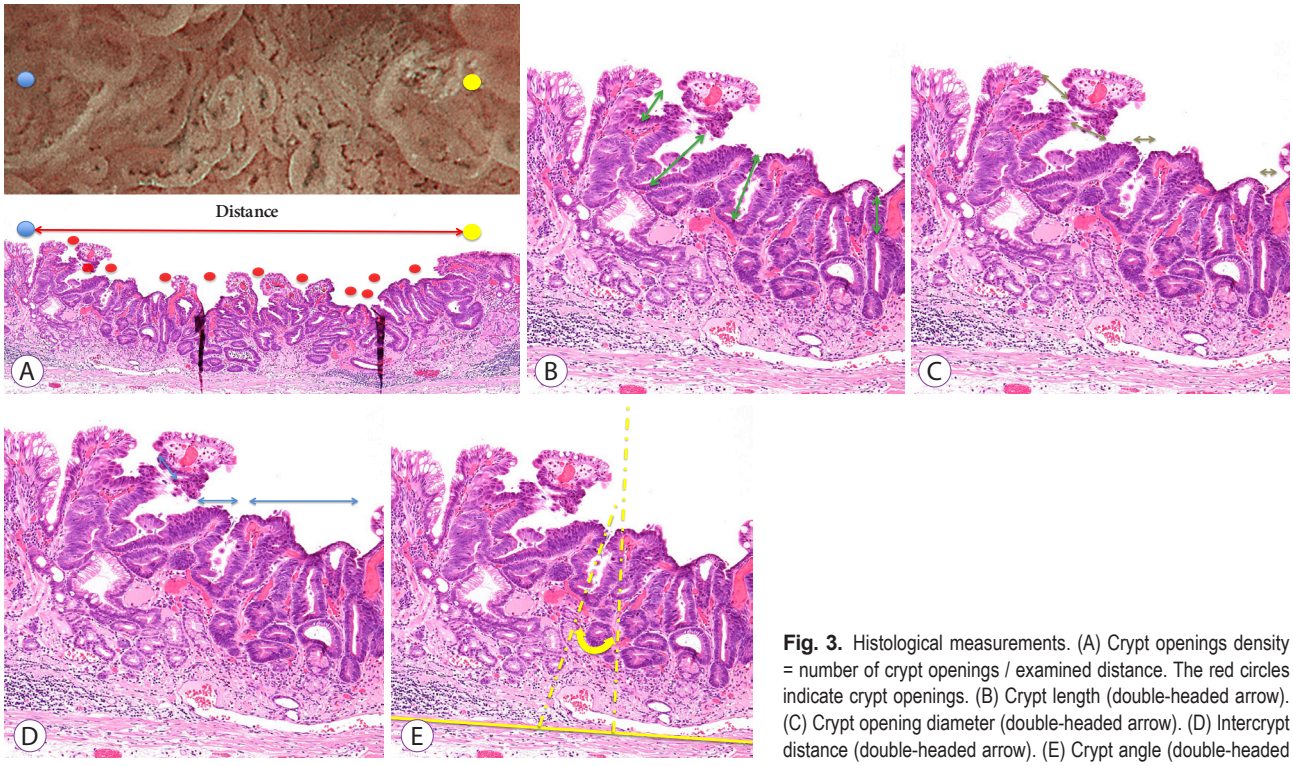

Fig. 3. Histological measurements. (A) Crypt openings density = number of crypt openings / examined distance. The red circles indicate crypt openings. (B) Crypt length (double-headed arrow). (C) Crypt opening diameter (double-headed arrow). (D) Intercrypt distance (double-headed arrow). (E) Crypt angle (double-headed arrow).

absent MSP and present MSP groups.

2) Differences in clinical pathology features between the absent MSP and present MSP groups.

Statistical analysis

Between-group statistical tests of the mean and median values for the continuous variables were performed using the Student's *t*-test and Mann–Whitney *U* test, respectively. Between-group statistical tests of frequencies were performed using Fisher's exact test and linear by linear association test. The Statistical Package for Social Science (SPSS) for Windows ver. 22 (IBM SPSS Co., Armok, NY, USA) was used for the statistical analyses.

RESULTS

Thirty-seven gastric epithelial neoplastic lesions fulfilled the inclusion criteria and did not meet any of the exclusion criteria followed in the study. One lesion was then excluded due to tissue crushing. Consequently, 36 lesions (32 adenocarcinomas and 4 adenomas) were included in the analysis.

The findings obtained by M-NBI showed that 17 lesions (42.7%) exhibited absent MSPs and 19 (52.8%) exhibited present MSPs.

Histological measurements for absent MSP and present MSP groups

Three typical lesions from the absent MSP group and one from the present MSP group are shown, along with their measurement values, in Fig. 4A-C.

The results of a comparison of the histological measurements in the absent MSP and present MSP groups were as follows. (1) The median (range) crypt opening density was 0.9 crypt openings/mm (0.0 to 3.0 crypt openings/mm) vs. 4.8 crypt openings/mm (1.88 to 9.33 crypt openings/mm), respectively ($p<0.001$). (2) The median crypt length (range) was 80.0 μm (0.0 to 140.0 μm) vs. 160 μm (55.7 to 415.3 μm), respectively ($p<0.001$). (3) The median crypt opening diameter (range) was 40.0 μm (0.0 to 80.0 μm) vs. 44.2 μm (22.5 to 100.0 μm), respectively ($p=0.09$). (4) The median intercrypt distance (range) was 572.5 μm (190.0 to 300.0 μm) vs. 166.7 μm (90.0 to 428.3 μm), respectively ($p<0.001$). (5) The median crypt angle (range) was 21.6 degrees (16.6 to 90.0 degrees) vs. 15.5 μm (7.3 to 28.7 degrees), respectively ($p<0.001$).

Clinical pathology features included in the analysis

In terms of age, sex, location, macroscopic type, and histological type, the absent MSP and present MSP groups differed only with respect to location, with the lesions tending to be present at lower locations in the present MSP group (Table 1). When examining the histological types, the two groups were

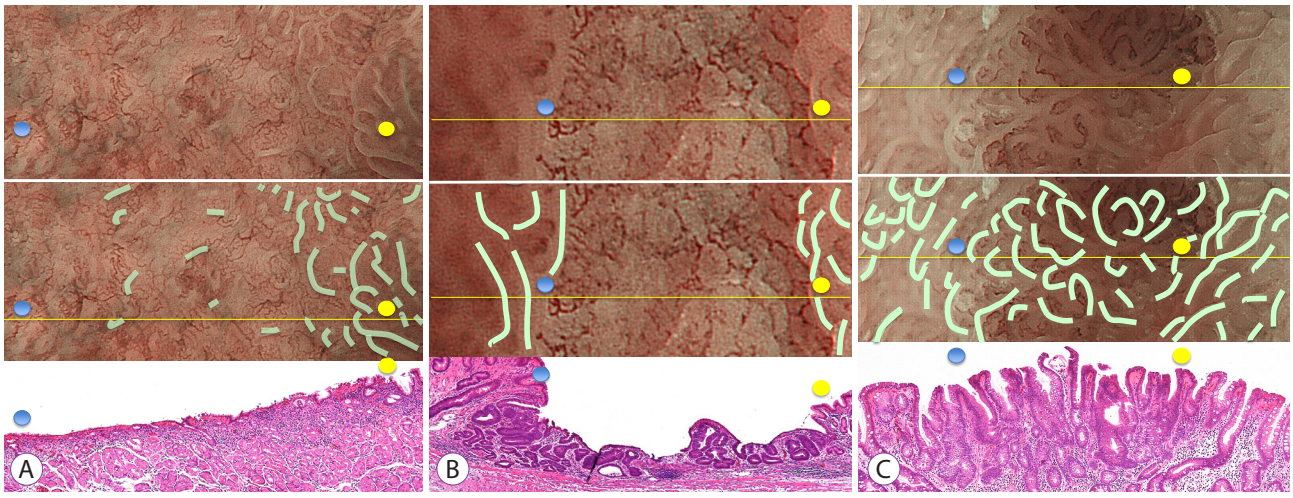

Fig. 4. Typical examples and histological measurements (mean±standard deviation for crypt length, crypt opening diameter, intercrypt distance, and crypt angle) for the absent microsurface pattern (MSP) and present MSP groups. (A) Example of early gastric cancer showing an absent MSP using magnifying endoscopy with narrow-band imaging (M-NBI). Histological findings indicated moderately to poorly differentiated adenocarcinomas. It's crypt opening density was 2 crypt openings/mm, crypt length was 80±87.5 μm, crypt opening diameter was 35.0±8.7 μm, intercrypt distance was 256.7±140.1 μm, and crypt angle was 15.5±20.9 degrees. (B) Example of early gastric cancer showing an absent MSP using M-NBI. Histological findings showed a well-differentiated adenocarcinoma. It's crypt opening density was 1.71 crypt openings/mm, crypt length was 100±25 μm, crypt opening diameter was 56.7±5.8 μm, intercrypt distance was 350±282.3 μm, and crypt angle was 27.3±19.6 degrees. (C) Example of early gastric cancer showing a present MSP. Histological findings demonstrated a well-differentiated adenocarcinoma. It's crypt opening density was 6.28 crypt openings/mm, crypt length was 224.5±101.3 μm, crypt opening diameter was 40.9±18.7 μm, intercrypt distance was 120±48.5 μm, and crypt angle was 12.5±12.5 degrees.

Table 1. Comparison of Clinical Pathology Features for Absent Microsurface Pattern and Present Microsurface Pattern Groups

	Absent MSP (*n*=17)	Present MSP (*n*=19)	*p*-value
Age, average (SD), yr	69±12.2	72±8.1	NS[a]
Sex, *n* (M:F)	12:5	16:3	NS[b]
Tumor size, mean (SD), mm	13.9±7.0	12.4±8.3	NS[a]
Tumor location, *n*			0.012[c]
Lower location	10	18	
Middle location	6	1	
Upper location	1	0	
Microscopic type, *n*			NS[c]
0-IIc	15	13	
0-IIa	2	4	
0-IIa + IIc	0	2	
Histological type, *n*			<0.001[c]
Poorly	6	0	
Moderately to poorly	2	1	
Very well to poorly	1	0	
Well to moderately	3	2	
Well	4	3	
Very well to well	1	7	
Very well	0	2	
Adenoma	0	4	

MSP, microsurface pattern; NS, not significant; SD, standard deviation.

[a]Student's *t*-test, [b]Fisher's exact test, [c]linear by linear association test.

compared with respect to lesions that included undifferentiated-type adenocarcinomas (*n*=10) and other lesions excluding adenomas (*n*=22), the ratio that included undifferentiated-type adenocarcinomas was significantly higher in the absent MSP group than in the present MSP group (*p*=0.007; Table 2).

Table 2. Frequency of Lesions that Included Undifferentiated-Type Adenocarcinomas and of Differentiated-Type Adenocarcinoma in Absent Microsurface Pattern and Present Microsurface Pattern Groups

	Undifferentiated (*n*=10)	Differentiated (*n*=22)	*p*-value
Absent MSP, *n* (%)	9 (90.0)	8 (36.4)	0.007
Present MSP, *n* (%)	1 (10.0)	14 (63.6)	

MSP, microsurface pattern.

DISCUSSION

The histological findings in this study showed that lesions exhibiting absent MSPs had lower crypt opening density, shorter crypt length, greater intercrypt distance, and larger crypt angle. The results obtained in this study represent the first reported results that describe the composition of the his-

topathological structure of epithelial neoplasms that exhibit an absent MSP, as determined by a one-to-one correspondence between magnifying endoscopy images obtained under constant viewing conditions and histopathological findings. Yao inferred that the mechanism by which the marginal crypt epithelium, a surface microstructure, is visualized involves backward scattering of projected light by the vertically arranged marginal crypt epithelium, with vertical accumulation of the backward scattering resulting in visualization of the whitish, semi-transparent marginal crypt epithelium (Fig. 5A).[15] Considering the results of the present study in light of this hypothesis, it was inferred that the marginal crypt epithelium is not visualized due to a low crypt opening density or a large intercrypt distance, resulting in a reduced number of crypts that cause backward scattering. This prevents visualization of the marginal crypt epithelium, and thus results in an absent MSP (Fig. 5B). In addition, if the crypt length is short or the crypt angle large, the vertical backward scattering accumulation may be inadequate, preventing visualization of the marginal crypt epithelium (Fig. 5C, D).

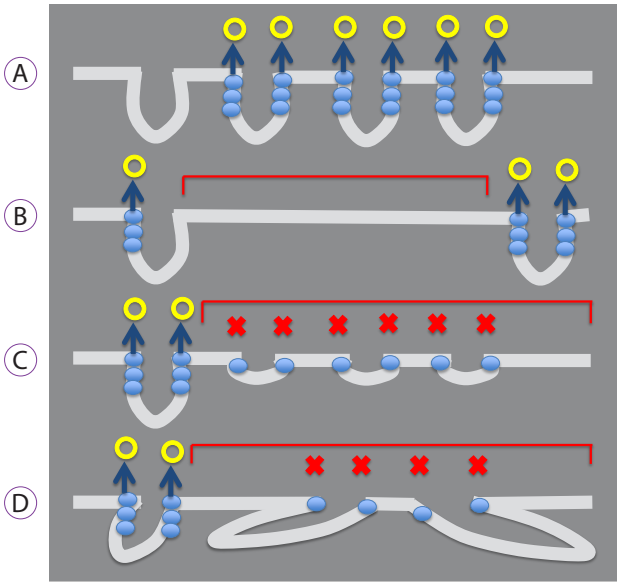

Fig. 5. Mechanisms by which the marginal crypt epithelium is visualized and not visualized. (A) Mechanism of visualization. Backward scattering caused by the marginal crypt epithelium (blue circle) is vertically integrated (blue arrow), and the epithelium is visualized (yellow circle). (B-D) Mechanisms that make visualization difficult. (B) If the crypt opening density is low or the intercrypt distance large, the number of crypts that cause backward scattering (blue circle) is reduced, resulting in the absent microsurface pattern (MSP; red square brackets). (C) If the crypt length is short or (D) the crypt angle is large (i.e., crypts run obliquely), the backward scatter (blue circle) does not integrate vertically. Consequently, the epithelium is not visualized as a white, belt-like structure (marginal crypt epithelium), resulting in the absent MSP (red square brackets).

Yagi et al. examined crypt depth and intercrypt distance after dividing lesions into three groups: (1) in which the marginal crypt epithelium could be observed, (2) in which it was difficult to observe, and (3) in which it could not be observed.[16] They reported that for marginal crypt epithelium that could not be observed or was difficult to observe, the intercrypt distance was short and crypt depth was shallow.[16] Although our results were similar for crypt depth, they differed for intercrypt distance. This difference may be due to differences in viewing conditions, the criteria for inclusion in the MSP group, and the lesions included in the study. If the magnification is low, the surface microstructure of some lesions is difficult to visualize when the crypts are densely arranged. However, we observed all lesions under the same condition of maximum magnification. Consequently, the marginal crypt epithelium was visualized, even in lesions with a high crypt density, and they were therefore assessed as a present MSP. Investigations that use images obtained under uniform viewing conditions, as in the present study, will likely provide results of greater reproducibility.

Kanesaka et al. reported a significantly higher proportion of undifferentiated carcinomas when 50% or more of the region of a lesion consisted of an absent MSP.[4] In this study, the frequency of undifferentiated-type carcinomas was significantly higher in the absent MSP group than in the present MSP group. However, differentiated-type carcinomas in the absent MSP group were found in eight lesions (47.1%). A potential reason for this unexpected increase in proportion is that most differentiated-type carcinomas exhibiting an absent MSP may have been included because only certain parts of the lesions were extracted and studied. Therefore, Kanesaka et al.[4] advocates that histological type diagnoses be performed on lesions where absent MSPs account for 50% or more of the entire lesion.

In contrast, a case of undifferentiated-type carcinoma was observed in the present MSP group. As reported by Phalanusitthepha et al., the stretch sign, an expansion of the area between crypts, is a finding specific to magnifying endoscopy observations in early-stage signet-ring cell carcinoma,[17] and lesions that do not exhibit absent MSPs may be included among undifferentiated-type tumors that are 2 cm or less in size, for which endoscopic submucosal dissection is indicated. In the present study as well, the findings obtained by M-NBI for small tumors associated with signet ring cells or undifferentiated-type cancer, primarily in the middle layer of the mucosa, were described as indicative of present MSP.

Consequently, a limitation of this study was that the magnifying endoscopy images were obtained at a precise maximum magnification, and lesions for which a reliable comparative

examination could be performed were sampled. Consequently, the large number of small carcinomas with relatively small lesions may have resulted from a bias in lesion selection. This study was a retrospective pilot study. Therefore, to resolve these problems, we are planning a prospective study that will include consecutive cases.

In conclusion, we demonstrated that the histological structure of lesions that exhibit absent MSP can, to a certain extent, be estimated. However, the parts observed by magnifying endoscopy are changes near the surface epithelium, and deeper changes cannot be seen directly. When an absent MSP site is seen, inferring the presence of a histological structure with features such as a low crypt opening density, short crypt length, greater intercrypt distance, and a large crypt angle is useful for accurate histological diagnosis by magnification endoscopy.

Conflicts of Interest

The authors have no potential conflicts of interest.

Funding

This study was funded by Central Research Institute for Endoscopy, Fukuoka University.

Acknowledgment

We would like to thank Dr Hisatomi Arima (Department of Preventive Medicine and Public Health, Fukuoka University, Fukuoka, Japan) for his constructive discussion regarding statistical analysis.

Author Contributions

Conceptualization: Kenshi Yao
Data curation: Kenta Chuman
Formal analysis: KC
Investigation: KC, Takashi Nagahama, Masaki Miyaoka, Haruhiko Takahashi, Kentaro Imamura, Rino Hasegawa, Toshiharu Ueki, Hiroshi Tanabe, Seiji Haraoka, Akinori Iwashita
Project administration: KY
Supervision: KY
Visualization: Takao Kanemitsu
Writing-original draft: KC
Writing-review&editing: KY

ORCID

Kenta Chuman: https://orcid.org/0000-0002-6653-6305
Kenshi Yao: https://orcid.org/0000-0003-0863-3649
Takao Kanemitsu: https://orcid.org/0000-0003-0581-2211
Takashi Nagahama: https://orcid.org/0000-0002-1692-9944
Masaki Miyaoka: https://orcid.org/0000-0002-4166-2372
Haruhiko Takahashi: https://orcid.org/0000-0001-6352-1741
Kentaro Imamura: https://orcid.org/0000-0001-6428-3677
Rino Hasegawa: https://orcid.org/0000-0002-3668-020X
Toshiharu Ueki: https://orcid.org/0000-0002-4142-5895
Hiroshi Tanabe: https://orcid.org/0000-0002-1301-719X
Seiji Haraoka: https://orcid.org/0000-0001-8995-9629
Akinori Iwashita: https://orcid.org/0000-0002-8095-5987

REFERENCES

1. Ezoe Y, Muto M, Uedo N, et al. Magnifying narrowband imaging is more accurate than conventional white-light imaging in diagnosis of gastric mucosal cancer. Gastroenterology 2011;141:2017-2025.e3.
2. Uedo N, Ishihara R, Iishi H, et al. A new method of diagnosing gastric intestinal metaplasia: narrow-band imaging with magnifying endoscopy. Endoscopy 2006;38:819-824.
3. Kanemitsu T, Yao K, Nagahama T, et al. The vessels within epithelial circle (VEC) pattern as visualized by magnifying endoscopy with narrow-band imaging (ME-NBI) is a useful marker for the diagnosis of papillary adenocarcinoma: a case-controlled study. Gastric Cancer 2014;17:469-477.
4. Kanesaka T, Sekikawa A, Tsumura T, et al. Absent microsurface pattern is characteristic of early gastric cancer of undifferentiated type: magnifying endoscopy with narrow-band imaging. Gastrointest Endosc 2014;80:1194-1198.e1.
5. Kanesaka T, Sekikawa A, Tsumura T, et al. Dense-type crypt opening seen on magnifying endoscopy with narrow-band imaging is a feature of gastric adenoma. Dig Endosc 2014;26:57-62.
6. Nakayoshi T, Tajiri H, Matsuda K, Kaise M, Ikegami M, Sasaki H. Magnifying endoscopy combined with narrow band imaging system for early gastric cancer: correlation of vascular pattern with histopathology (including video). Endoscopy 2004;36:1080-1084.
7. Doyama H, Yoshida N, Tsuyama S, et al. The "white globe appearance" (WGA): a novel marker for a correct diagnosis of early gastric cancer by magnifying endoscopy with narrow-band imaging (M-NBI). Endosc Int Open 2015;3:E120-E124.
8. Yagi K, Nozawa Y, Endou S, Nakamura A. Diagnosis of early gastric cancer by magnifying endoscopy with NBI from viewpoint of histological imaging: mucosal patterning in terms of white zone visibility and its relationship to histology. Diagn Ther Endosc 2012;2012:954809.
9. Kobayashi M, Takeuchi M, Ajioka Y, et al. Mucin phenotype and narrow-band imaging with magnifying endoscopy for differentiated-type mucosal gastric cancer. J Gastroenterol 2011;46:1064-1070.
10. Uchita K, Yao K, Uedo N, et al. Highest power magnification with narrow-band imaging is useful for improving diagnostic performance for endoscopic delineation of early gastric cancers. BMC Gastroenterol 2015;15:155.
11. Yao K, Imamura K, Yamaoka R, et al. [How to construct for gastrointrestinal imaging]. Stomach and Intestine 2016;51:1131-1148.
12. Doyama H, Nakanishi H, Yoshida N, Takeda Y, Tsuyama S, Kurumaya H. [Techniques for comparing endoscopic and histopathological results in early gastric cancer]. Stomach and Intestine 2016;51:1203-1210.
13. Yao K, Anagnostopoulos GK, Ragunath K. Magnifying endoscopy for diagnosing and delineating early gastric cancer. Endoscopy 2009;41:462-467.
14. Japanese Gastric Cancer Association. Japanese classification of gastric carcinoma: 3rd English edition. Gastric Cancer 2011;14:101-112.
15. Yao K. Zoom gastroscopy: magnifying endoscopy in the stomach. Tokyo: Springer Japan; 2014.
16. Yagi K, Saka A, Nozawa Y, Nakamura A, Umezu H. [The characteristic finding of histological mixed type of gastric adenocarcinoma in magnifying endoscopy]. Stomach and Intestine 2013;48:1609-1618.
17. Phalanusitthepha C, Grimes KL, Ikeda H, et al. Endoscopic features of early-stage signet-ring-cell carcinoma of the stomach. World J Gastrointest Endosc 2015;7:741-746.